Smart Structures and Systems, *Vol. 13, No. 1 (2014) 001-024*
DOI: http://dx.doi.org/10.12989/sss.2014.13.1.001

Application of shear deformation theory for two dimensional electro-elastic analysis of a FGP cylinder

M. Arefi[*1] and G.H. Rahimi[2a]

[1]*Department of Solid Mechanic, Faculty of Mechanical Engineering, University of Kashan, Kashan 87317-51167, Iran*
[2]*Department of Mechanical engineering, Tarbiat Modares University, Tehran 14115-143, Iran*

(Received July 31, 2012, Revised December 26, 2012, Accepted February 19, 2013)

Abstract. The present study deals with two dimensional electro-elastic analysis of a functionally graded piezoelectric (FGP) cylinder under internal pressure. Energy method and first order shear deformation theory (FSDT) are employed for this purpose. All mechanical and electrical properties except Poisson ratio are considered as a power function along the radial direction. The cylinder is subjected to uniform internal pressure. By supposing two dimensional displacement and electric potential fields along the radial and axial direction, the governing differential equations can be derived in terms of unknown electrical and mechanical functions. Homogeneous solution can be obtained by imposing the appropriate mechanical and electrical boundary conditions. This proposed solution has capability to solve the cylinder structure with arbitrary boundary conditions. The previous solutions have been proposed for the problem with simple boundary conditions (simply supported cylinder) by using the routine functions such as trigonometric functions. The axial distribution of the axial displacement, radial displacement and electric potential of the cylinder can be presented as the important results of this paper for various non homogeneous indexes. This paper evaluates the effect of a local support on the distribution of mechanical and electrical components. This investigation indicates that a support has important influence on the distribution of mechanical and electrical components rather than a cylinder with ignoring the effect of the supports. Obtained results using present method at regions that are adequate far from two ends of the cylinder can be compared with previous results (plane elasticity and one dimensional first order shear deformation theories).

Keywords: piezoelectric; pressure; cylindrical shell; first order shear deformation theory; energy method

1. Introduction

Piezoelectric materials were discovered in India. These materials have tendency to absorb tiny particles when heated. Quartz has been known as the first piezoelectric material. The piezoelectric structures can be electrified under mechanical loads and conversely can be deformed under external electric field. These two effects can be applied in sensor and actuator applications. The piezoelectric effect was scientifically discovered by Pierre and Jacques Curie in 1880. Piezoelectric structures are very applicable in industrial systems as actuator or sensor in various

∗Corresponding author, Assistant Professor, E-mail: arefi@kashanu.ac.ir & arefi63@gmail.com
[a]Professor, E-mail: rahimi_gh@modares.ac.ir.

http://www.techno-press.org/?journal=sss&subpage=8 ISSN: 1738-1584 (Print), 1738-1991 (Online)

geometries such as disk; cylinder and shell. For many applicable conditions, it is appropriate to investigate the relation between the applied loads, electric field and displacement in the piezoelectric structures such as cylindrical shell.

In order to control the distribution of the displacement or electric potential in the piezoelectric structures, functionally graded piezoelectric material (FGPM) can be used. The properties of this material vary continuously along the coordinate system. These materials were proposed for the first time by a Japanese group of material scientist. For many advantageous properties, these materials can be used in vigorous environments with abruptly gradient of pressure and temperature. A brief literature of FSDT for shell analyses is presented as follows:

One of the most applicable structures in the mechanical engineering is the shells. Ratio of thickness with respect to other dimensions such as radius of curvature for the shells is small. As the general case, they can be classified to two classes i.e., thin and thick shells. Thin shells are applicable for bearing the membrane and in-plane forces. Membrane theory can be used to utilize this class of the shells. The second class of shells are the thick shells. For this group of shells, the deformation of shell includes displacement of middle surface and rotation about middle surface of the shell. Thick shells can be applied to undergo bending and stretching force, simultaneously.

The exact solution of a thick walled cylinder under inner and outer pressures was presented by Lame (Timoshenko 1976). It has been supposed that the cylinder to be axisymmetric and isotropic. Naghdi and Cooper (1956) applied the theory of shear deformation for studying the elastic waves in a cylindrical shell. FSDT for analysis of an isotropic cylinder was presented for the first time by Mirsky and Hermann (1958).

Researches on the thermal and vibration analysis of functionally graded material (FGM) were started since first years of 1990s (Yamanouchi *et al.* 1990). Tutuncu and Ozturk (2001) presented exact solution of functionally graded (FG) spherical and cylindrical pressure vessels. Jabbari et al (2002) analyzed thermo-elastic analysis of a FG cylinder under thermal and mechanical loads. It was supposed that the material properties vary as a power function in terms of radial coordinate system. Mechanical and electrical analyses of a spherical shell were investigated by Chen *et al.* (2002). An analytical model for free vibration analysis of a cylindrical shell under mechanical and electrical loads was proposed by Liu *et al.* (2002). Shai *et al.* (2004) presented the exact solution of a functionally graded piezoelectric (FGP) clamped beam. Mindlin's theory was employed for this analysis and a sinusoidal function was used for simulation of the electric potential distribution. Peng-Fei *et al.* (2004) studied piezoelectric analysis of a cylindrical shell. Wu *et al.* (2005) investigated the elastic stability of a FG cylinder. They employed shell Donnell's theory to derive the strain-deformation relations.

Shao (2005) performed thermo-elastic analysis of a thick walled cylinder under mechanical and thermal loads. The cylinder has been divided into many annular sub cylinders in the radial direction. Exact solution of a FGP cylinder under bending was studied by Lu *et al.* (2005). Dai *et al.* (2007) performed electro-magneto-elastic behavior of the FGP cylindrical and spherical pressure vessels. Exact solution of an infinitely long magneto-elastic hollow cylinder and solid rotating cylinder polarized and magnetized radially, was presented by Babaei *et al.* (2008a). Electro-elastic analysis of a FGP rotating hollow shaft was studied where the variation of material properties was assumed to follow a power law along the radial direction by Babaei and Chen (2008b). The effect of non-homogeneity has been considered on the mechanical and electrical components. The cylinder was supposed orthotropic. They investigated the effect of angular velocity on the hoop and radial stresses. Jabbari *et al.* (2009) analyzed two dimensional thermo-elastic analysis of a FG cylinder under thermal and mechanical loads. They solved the

problem using the pre-defined displacement field. The solution method was applicable for simply supported cylinder, only. The present paper proposes a novel method for solution of cylinder with different boundary conditions. Qian *et al*. (2008) used exponential variation functionality for a FGP substrate in order to study behavior of transverse surface waves using analytical technique. The influence of the initial stress was discussed on the distributions of the mechanical displacement and shear stresses along the thickness direction by Qian *et al*. (2009).

Khoshgoftar et al (2009) studied thermo-elastic analysis of the FGP cylindrical pressure vessels. They supposed that all mechanical and electrical properties could be varied as a power function. Qian *et al*. (2009a, b, c) studied the effect of in-homogeneity on the vibration modes of a FGPM. They indicated that in-homogeneity has significant effect on the fundamental mode and long waves and has negligible effect on the higher order modes and short waves. The transient thermo-piezoelectric response of a radially polarized FG hollow cylinder was investigated by Babaei and Chen (2010a). The effect of transient thermal loading has been investigated on the different results. They also presented a one-dimensional thermo-piezo-electricity analysis of a FG medium excited by a moving heat source (Babaei and Chen 2010b).

Thermo-elastic analysis of a FG cylinder was analytically investigated by Arefi and Rahimi (2010). They used the FSDT for simulation of displacement components of a FG structure. The achieved results were compared with those results that have been derived by using the plane elasticity theory. Sheng and Wang (2010) employed FSDT for evaluation of approximate solution of the FG laminated piezoelectric cylindrical shells under thermal shock and moving mechanical loads. Hamilton's principle was used for derivation of governing equation of the system. Babaei and Chen (2010c) presented one-dimensional heat conduction analysis of a FG hollow cylinder in the radial direction in the Laplace domain for hyperbolic heat conduction.

The effect of variable material properties on the electro-mechanical behavior of a FGP sphere was analytically investigated by Wang and Xu (2010). The spherical shell was subjected to mechanical and electrical loads and was polarized in radial direction. The closed form solution of the second order ordinary differential equation with variable coefficient was obtained using the Frobenius series method. The material properties were assumed to be exponential function of the radial direction. Thermoelastic solution of a FG cylindrical shell with piezoelectric layers was studied by Alibeigloo (2010). The assumed problem was solved analytically using the Navier's solution. They investigated the effect of mechanical and electrical boundary conditions on the response of the system. The assumed stress and displacement functions were used for solution of equilibrium equations. The assumed functions were applicable for one type of boundary conditions (simply supported). Because of this incomplete study of that paper, the present paper proposed the comprehensive governing differential equations and solved that analytically with every simple and complex boundary condition.

Dynamic response of a rotating radially polarized FGP hollow cylinder is investigated under a constant magnetic field and thermo-electro-mechanical loading by Akbarzadeh *et al*. (2011a). The effect of various mechanical, electrical and thermal parameters has been studied on thermo-electro-magneto-elastic behavior of the hollow cylinder.

The effects of the covering dielectric layer thickness and material gradient was investigated on the Love waves and other parameters such as phase velocity, group velocity for a FGPM structure by Qian *et al*. (2011a, b). Laplace transform and successive decoupling method have been employed for dynamic response of a FGPM rod of exponentially varying excited by a moving heat source by Akbarzadeh *et al*. (2011b). A functionally graded piezoelectric rotating cylinder as mechanical sensor under pressure and thermal loads was analytically investigated by Rahimi *et al*.

(2011) for evaluation of angular velocity of rotary devices. Arefi and Rahimi (2011a, b, c, 2012a, b, c, d, e, f) investigated on the general formulation, thermo-piezo-magnetic and nonlinear analyses of piezoelectric structures by using the energy method.

The present paper proposed an analytical method based on the FSDT and using energy functional for the two dimensional analysis of a FGP cylinder with different mechanical and electrical boundary conditions. This method simulates the effect of end supports on the electro-elastic behavior of a FGP cylinder using FSDT. The previous papers have not truly considered the effect of the end supports on the cylinder (Jabbari *et al*. 2009).

2. Formulation

Two dimensional electro-elastic analysis of a FGP cylinder is studied in the present work. For analysis of a solid structure, two methods may be employed. Equilibrium and energy methods are two appropriate methods for analysis of a solid structure. Every method has whose special advantageous. For example, energy method has capability to formulate two dimensional analysis of a FG hollow structure with different boundary conditions. In order to obtain the general formulation of a FGP cylinder in general state, the energy method can be employed in the present study. Furthermore FSDT is employed for simulation of the deformations.

Equilibrium method can be applied for pre-defined functions. For example Jabbari *et al*. (2009) studied two dimensional behavior of the FG cylinder with simply-simply supported. More complicated boundary conditions cannot be simulated using a single and straight function in order to satisfy two navier equations. This incomplete solution may be observed in Alibeigloo study (2010).

The present study focuses on FSDT for simulation of the deformations in a piezoelectric structure. This theory uses the classic solution of the pressure vessels. Based on the classic solution of the pressure vessels, radial displacement *u(r)* of an axisymmetric cylinder in the radial coordinate system is (Timoshenko 1976, Arefi and Rahimi 2010)

$$u(r) = c_1 r + \frac{c_2}{r} \tag{1}$$

This solution is well-known as Lame's solution. In Eq. (1), *r* is distance of every element with respect to axis of the cylinder. For a cylinder, this distance can be expressed as summation of the radius of mid-surface *R* and distance of every element with respect to mid-surface ρ as follows

$$\mathrm{r}=\mathrm{R}+\rho \tag{2}$$

By substitution of Eq. (2) into Eq. (1) and using the Taylor expansion, we'll have

$$u = c_1(\mathrm{R}+\rho) + \frac{c_2}{\mathrm{R}+\rho} = c_0' + c_1'\rho + \ldots \tag{3}$$

This formulation (Eq. (3)) is known as FSDT. Based on this theory, each deformation component may be expressed by two variables including the displacement and rotation. For a symmetric cylindrical shell, the radial and axial components of deformation may be considered as follows

$$\begin{Bmatrix} u_z \\ w_r \end{Bmatrix} = \begin{Bmatrix} u \\ w \end{Bmatrix} + \rho \begin{Bmatrix} \psi_z \\ \psi_r \end{Bmatrix} \tag{4}$$

where, u_z , w_r are the axial and radial components of deformation, respectively. u, w, ψ_z, ψ_r are the functions of axial component of coordinate system (*z*), only. By considering the Eq. (4), the strain components are (Arefi and Rahimi 2010):

$$\begin{cases} \varepsilon_r = \dfrac{\partial w_r}{\partial \rho} = \psi_r \\ \varepsilon_\theta = \dfrac{w_r}{r} = \dfrac{w + \rho \psi_r}{R + \rho} \\ \varepsilon_z = \dfrac{\partial u_z}{\partial z} = \dfrac{\partial u}{\partial z} + \rho \dfrac{\partial \psi_z}{\partial z} \\ \gamma_{rz} = 2 \times \varepsilon_{rz} = \dfrac{\partial u_z}{\partial \rho} + \dfrac{\partial w_r}{\partial z} = \psi_z + \dfrac{\partial w}{\partial z} + \rho \dfrac{\partial \psi_r}{\partial z} \end{cases} \tag{5}$$

The comprehensive stress-strain relations for a piezoelectric structure are expressed (Khoshgoftar *et al*. 2009, Arefi and Rahimi 2011, 2012)

$$\sigma_{ij} = \sigma_{ij})_m + \sigma_{ij})_e = C_{ijkl}\varepsilon_{kl} - e_{ijk}E_k \rightarrow$$
$$\begin{cases} \sigma_{rr} = C_{rrzz}\varepsilon_{zz} + C_{rrrr}\varepsilon_{rr} + C_{rr\theta\theta}\varepsilon_{\theta\theta} - e_{rrz}E_z - e_{rr\theta}E_\theta - e_{zzr}E_r \\ \sigma_{\theta\theta} = C_{\theta\theta zz}\varepsilon_{zz} + C_{\theta\theta rr}\varepsilon_{rr} + C_{\theta\theta\theta\theta}\varepsilon_{\theta\theta} - e_{\theta\theta z}E_z - e_{\theta\theta\theta}E_\theta - e_{\theta\theta r}E_r \\ \sigma_{zz} = C_{zzzz}\varepsilon_{zz} + C_{zzrr}\varepsilon_{rr} + C_{zz\theta\theta}\varepsilon_{\theta\theta} - e_{zzz}E_z - e_{zz\theta}E_\theta - e_{zzr}E_r \\ \sigma_{rz} = C_{rzrz}\varepsilon_{rz} \end{cases} \tag{6}$$

where, C_{ijkl}, e_{ijk} are elastic stiffness and piezoelectric coefficients, $\sigma_{ij}, \varepsilon_{kl}, E_k$ are the stress, strain and electric field components, respectively. In this section, it is appropriate to define the components of the electric field. By employing an electric potential $\phi(r, \theta, z)$ in a piezoelectric structure, the electric field can be defined as:

$$\vec{E} = -\vec{\nabla}\phi \rightarrow \{E_r, E_\theta, E_z\} = -\left\{\frac{\partial \phi}{\partial r}, \frac{1}{r}\frac{\partial \phi}{\partial \theta}, \frac{\partial \phi}{\partial z}\right\} \tag{7}$$

Due to symmetric condition $\dfrac{\partial}{\partial \theta} = 0$ and considering $\dfrac{\partial}{\partial r} = \dfrac{\partial}{\partial \rho}$, the electric field components can be obtained as follows

$$E_r = -\frac{\partial \phi}{\partial \rho}, E_\theta = 0, E_z = -\frac{\partial \phi}{\partial z} \tag{8}$$

By selection of appropriate electric potential ϕ, Eq. (6) can be completed. Based on the

assumption and results of the previous papers (Khoshgoftar *et al*. 2009, Sheng and Wang 2010) the electric potential function may be supposed as a quadratic function along the thickness direction and an unknown function along the axial direction

$$\phi(z,\rho)=\phi_0(z)+\rho\phi_1(z)+\rho^2\phi_2(z) \tag{9}$$

By substitution of Eq. (9) into Eq. (7), the electric field can be expressed as follows

$$\vec{E}=-\left\{\phi_1(z)+2\rho\phi_2(z),0,\frac{\partial\phi_0}{\partial z}+\rho\frac{\partial\phi_1}{\partial z}+\rho^2\frac{\partial\phi_2}{\partial z}\right\} \tag{10}$$

For an electro-mechanical system, the electric displacement or electric flux D_i may be defined as a linear combination of the strain and electric field as follows (Khoshgoftar *et al*. 2009, Arefi and Rahimi 2011, 2012)

$$\begin{aligned}&D_i=e_{ijk}\varepsilon_{jk}+\eta_{ik}E_k\rightarrow\\&\begin{cases}D_r=e_{rzz}\varepsilon_z+e_{rrr}\varepsilon_r+e_{r\theta\theta}\varepsilon_\theta+\eta_{rz}E_z+\eta_{rr}E_r\\D_\theta=e_{\theta zz}\varepsilon_z+e_{\theta rr}\varepsilon_r+e_{\theta\theta\theta}\varepsilon_\theta+\eta_{\theta z}E_z+\eta_{\theta r}E_r\\D_z=e_{zzz}\varepsilon_z+e_{zzr}\varepsilon_r+e_{z\theta\theta}\varepsilon_\theta+\eta_{zz}E_z+\eta_{zr}E_r\end{cases}\end{aligned} \tag{11}$$

where, D_i , η_{ik} are dielectric coefficients and electric displacement components. By recalling the components of the stresses, strains, electric field and electric displacements (Eqs. (5), (10), (11), and (12)), the energy equation per unit volume may be obtained. Total energy includes the mechanical and electrical energies. Mechanical energy is equal to the half of multiplying the stress tensor components in the corresponding strain tensor components. Electrical energy is equal to the half of multiplying the electric displacement tensor in the corresponding electric field tensor. Therefore energy per unit volume ($\bar{u}$) may be obtained as follows

$$\begin{aligned}&\bar{u}=\frac{1}{2}[\{\varepsilon\}^T\{\sigma\}-\{E\}^T\{D\}]\\&\bar{u}=\frac{1}{2}[\{\sigma_z\varepsilon_z+\sigma_z\varepsilon_z+\sigma_t\varepsilon_t+\tau_{xz}\gamma_{xz}\}-E_xD_x-E_zD_z-E_tD_t]=\\&\frac{1}{2}[[C_{rrzz}\varepsilon_{zz}+C_{rrrr}\varepsilon_{rr}+C_{rr\theta\theta}\varepsilon_{\theta\theta}-e_{rrz}E_z-e_{zzr}E_r]\varepsilon_r\\&+[C_{\theta\theta zz}\varepsilon_{zz}+C_{\theta\theta rr}\varepsilon_{rr}+C_{\theta\theta\theta\theta}\varepsilon_{\theta\theta}-e_{\theta\theta z}E_z-e_{\theta\theta r}E_r]\varepsilon_\theta\\&+[C_{zzzz}\varepsilon_{zz}+C_{zzrr}\varepsilon_{rr}+C_{zz\theta\theta}\varepsilon_{\theta\theta}-e_{zzz}E_z-e_{zzr}E_r]\varepsilon_z+[C_{rzrz}\gamma_{rz}]\gamma_{rz}\\&-E_z[e_{zzz}\varepsilon_z+e_{zzr}\varepsilon_r+e_{z\theta\theta}\varepsilon_\theta+\eta_{zz}E_z+\eta_{zr}E_r]-E_r[e_{rzz}\varepsilon_z+e_{rrr}\varepsilon_r+e_{r\theta\theta}\varepsilon_\theta+\eta_{rz}E_z+\eta_{rr}E_r]\end{aligned} \tag{12}$$

The total energy must be evaluated by integration of Eq. (12) on the volume of the cylinder. The volume element of the cylinder is $2\pi(R+\rho)drdz$. Therefore, total energy of the system is:

$$U = 2\pi \int_0^L \int_{-\frac{h}{2}}^{\frac{h}{2}} (R+\rho)\bar{u}d\rho dz = \int_0^L F_1(u, w, \psi_z, \psi_r, \phi_0, \phi_1, \phi_2, z)dz \tag{13}$$

where, *h* is the thickness of the cylinder. The functional of the system $F(u, w, \psi_x, \psi_z, \phi_0, \phi_1, \phi_2, x)$ can be obtained as follows

$$\frac{F_1}{\pi} = F(u, w, \psi_z, \psi_r, \phi_0, \phi_1, \phi_2, z) = 2\int_{-\frac{h}{2}}^{\frac{h}{2}} \bar{u}(R+\rho)d\rho \tag{14}$$

$F(u, w, \psi_z, \psi_r, \phi_0, \phi_1, \phi_2, z)$ can be decomposed into three types of terms based on the different material properties as follows

$$F(u, w, \psi_z, \psi_r, \phi_0, \phi_1, \phi_2, z) = \mathrm{U_S}(z) + \mathrm{U_{Piezo}}(z) - \mathrm{U_{Die}}(z) \tag{15}$$

Functional of the system include strain energy $\mathrm{U_S}(z)$, piezoelectric energy $\mathrm{U_{Piezo}}(z)$ and dielectric energy $\mathrm{U_{Die}}(z)$.

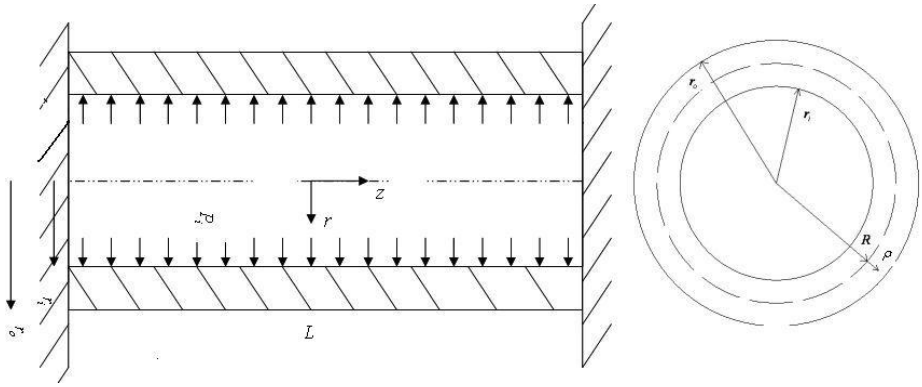

Fig. 1 The schematic figure of a FGP cylinder under mechanical and electrical loads

2.1. Definition of the external works

External works are included energy of internal and external pressures or energy of body forces such as centrifugal force. In this paper, internal and external pressures are considered in formulation. Energy of internal and external pressures is equal to multiplying the pressure in the radial deformation of the inner and outer surface of the cylinder, respectively. Inner pressure applies in the same direction of the deformation; conversely, outer pressure applies in the opposite direction of the deformation. Eq. (16) indicates work that is performed by the internal and external pressures. Fig. 1 shows the schematic figure of the cylindrical pressure vessel. In the present paper,

only internal pressure is considered in applied problem (Arefi and Rahimi 2010).

$$W_1 = \int_0^{2\pi} \int_0^{l} +P_i(w_{z=-h/2})dzd\theta = \int_0^{2\pi} \int_0^{l} +P_i(R-\frac{h}{2})(w-\frac{h}{2}\psi_r)dzd\theta \rightarrow$$
$$\frac{W_1}{\pi} = 2\int_0^{l} P_i(R-\frac{h}{2})wdz + 2\int_0^{l} \frac{h}{2}(-P_i(R-\frac{h}{2}))\psi_r dz = \int_0^{l}[f_1 w + f_2\psi_r]dz = \int_0^{l} W_1^{'}dz \tag{16}$$
$$f_1 = 2P_i(R-\frac{h}{2}), f_2 = h(-P_i(R-\frac{h}{2}))$$

2.2. Variation of the energy equation

Total energy of the system may be obtained by subtraction of Eq. (15) from Eq. (16) as follows

$$F(u,w,\psi_z,\psi_r,\phi_0,\phi_1,\phi_2,z) = \mathrm{U_S}(z) + \mathrm{U_{Piezo}}(z) - \mathrm{U_{Die}}(z) - \mathrm{W_1^{'}} \tag{17}$$

Every terms of above functional $\mathrm{U_S}(z), \mathrm{U_{Piezo}}(z), \mathrm{U_{Die}}(z)$ are demonstrated in the appendices (Appendix A, B, C).

Eq. (17) includes seven functions. By using Euler equation, variation of Eq. (17) can be expressed as follows (Arefi and Rahimi 2010)

$$\frac{\partial F}{\partial Q_i} - \frac{\partial}{\partial z}\left(\frac{\partial F}{\partial(\frac{\partial Q_i}{\partial z})}\right) = 0 \quad Q_i = u, w, \psi_z, \psi_r, \phi_0, \phi_1, \phi_2 \tag{18}$$

Using the Euler equation, final governing differential equation of system in the matrix form is

$$[G_1]_{7\times7}\frac{d^2}{dx^2}\{X\} + [G_2]_{7\times7}\frac{d}{dx}\{X\} + [G_3]_{7\times7}\{X\} = \{F\}_{7\times1}$$
$$\{X\} = \{u \quad \psi_z \quad w \quad \psi_r \quad \phi_0 \quad \phi_1 \quad \phi_2\}^T \tag{19}$$

where matrices G_i, F are functions of A_i, C_i, D_i and are demonstrated in the appendices (Appendix D, E, F, G).

2.3. Presentation of governing equations in terms of resultant of stress and electric displacement

The governing equations (Eq. (19)) can be expressed in terms of resultant of stress and electric displacement. Primarily, it is appropriate to introduce resultant of forces and moments and electric displacement as follows

$$
\begin{aligned}
&N_z=\int_{-\frac{h}{2}}^{+\frac{h}{2}}\sigma_z(1+\frac{\rho}{R})d\rho,\quad N_\theta=\int_{-\frac{h}{2}}^{+\frac{h}{2}}\sigma_\theta d\rho,\quad N_r=\int_{-\frac{h}{2}}^{+\frac{h}{2}}\sigma_r(1+\frac{\rho}{R})d\rho, M_\theta=\int_{-\frac{h}{2}}^{+\frac{h}{2}}\sigma_\theta\rho d\rho\\
&M_z=\int_{-\frac{h}{2}}^{+\frac{h}{2}}\sigma_z(1+\frac{\rho}{R})\rho d\rho,\quad M_{rz}=\int_{-\frac{h}{2}}^{+\frac{h}{2}}\rho\tau_{rz}(1+\frac{\rho}{R})d\rho, Q_r=\int_{-\frac{h}{2}}^{+\frac{h}{2}}(1+\frac{\rho}{R})\tau_{rz}d\rho\\
&d_{z1}=\int_{-\frac{h}{2}}^{+\frac{h}{2}}(R+\rho)D_z d\rho,\quad d_{z2}=\int_{-\frac{h}{2}}^{+\frac{h}{2}}\rho(R+\rho)D_z d\rho,\quad d_{z3}=\int_{-\frac{h}{2}}^{+\frac{h}{2}}\rho^2(R+\rho)D_z d\rho\\
&d_{r1}=\int_{-\frac{h}{2}}^{+\frac{h}{2}}(R+\rho)D_r d\rho,\quad d_{r2}=\int_{-\frac{h}{2}}^{+\frac{h}{2}}\rho(R+\rho)D_r d\rho
\end{aligned}
\tag{20}
$$

After performing long mathematic operations on the Eq. (19) with considering the presented matrices in appendices, we have seven Equilibrium and Maxwell equation in terms of resultant of forces, moments and electric displacement as follows

$$
\begin{cases}
\dfrac{\partial(RN_z)}{\partial z}=0\\
RQ_r-\dfrac{\partial}{\partial z}[RM_z]=0\\
N_\theta-\dfrac{\partial}{\partial z}[RQ_r]=\dfrac{f_1}{2}\\
RN_r+M_\theta-\dfrac{\partial}{\partial x}[RM_{rz}]=\dfrac{f_2}{2}\\
\dfrac{\partial d_{z1}}{\partial z}=0\\
d_{r1}-\dfrac{\partial d_{z2}}{\partial z}=0\\
2d_{r2}-\dfrac{\partial d_{z3}}{\partial z}=0
\end{cases}
\tag{21}
$$

These relations are presented for the first time. It is obvious that with ignoring the piezoelectric effect, the governing equations convert to governing equations of a pressurized FG cylinder that have been derived in the literature (Arefi and Rahimi 2010).

3. Two dimensional solution of a FGP cylinder

The important objective of this study is to investigate the effect of end supports on the response of the cylinder. For attaining to this purpose, it is inevitable to obtain the homogeneous solution of Eq. (19). Homogeneous solution of this problem includes fourteen constants of integration. These constants can be obtained by considering the natural boundary condition of two ends of the cylinder. Homogeneous solution of Eq. (19) in the general form is (subscript *h* shows that this solution is a homogeneous solution)

$$X_h{}^j = \sum_{i=1}^{14} c_i v^i{}_j e^{m_i z} \tag{22}$$

where, j indicates the number of unknown functions. For example $X^1 = u, ... X^7 = \phi_2$ .Eq. (22) in the extended form is

$$\{X\}_h = \begin{bmatrix} u \\ w \\ \psi_z \\ \psi_r \\ \phi_0 \\ \phi_1 \\ \phi_2 \end{bmatrix} = \begin{bmatrix} v^1_1 & v^2_1 & v^3_1 & v^4_1 & v^5_1 & v^6_1 & v^7_1 & v^8_1 & v^9_1 & v^{10}_1 & v^{11}_1 & v^{12}_1 & v^{13}_1 & v^{14}_1 \\ v^1_2 & v^2_2 & v^3_2 & v^4_2 & v^5_2 & v^6_2 & v^7_2 & v^8_2 & v^9_2 & v^{10}_2 & v^{11}_2 & v^{12}_2 & v^{13}_2 & v^{14}_2 \\ v^1_3 & v^2_3 & v^3_3 & v^4_3 & v^5_3 & v^6_3 & v^7_3 & v^8_3 & v^9_3 & v^{10}_3 & v^{11}_3 & v^{12}_3 & v^{13}_3 & v^{14}_3 \\ v^1_4 & v^2_4 & v^3_4 & v^4_4 & v^5_4 & v^6_4 & v^7_4 & v^8_4 & v^9_4 & v^{10}_4 & v^{11}_4 & v^{12}_4 & v^{13}_4 & v^{14}_4 \\ v^1_5 & v^2_5 & v^3_5 & v^4_5 & v^5_5 & v^6_5 & v^7_5 & v^8_5 & v^9_5 & v^{10}_5 & v^{11}_5 & v^{12}_5 & v^{13}_5 & v^{14}_5 \\ v^1_6 & v^2_6 & v^3_6 & v^4_6 & v^5_6 & v^6_6 & v^7_6 & v^8_6 & v^9_6 & v^{10}_6 & v^{11}_6 & v^{12}_6 & v^{13}_6 & v^{14}_6 \\ v^1_7 & v^2_7 & v^3_7 & v^4_7 & v^5_7 & v^6_7 & v^7_7 & v^8_7 & v^9_7 & v^{10}_7 & v^{11}_7 & v^{12}_7 & v^{13}_7 & v^{14}_7 \end{bmatrix} \begin{bmatrix} c_1 e^{m_1 z} \\ c_2 e^{m_2 z} \\ c_3 e^{m_3 z} \\ c_4 e^{m_4 z} \\ c_5 e^{m_5 z} \\ c_6 e^{m_6 z} \\ c_7 e^{m_7 z} \\ c_8 e^{m_8 z} \\ c_9 e^{m_9 z} \\ c_{10} e^{m_{10} z} \\ c_{11} e^{m_{11} z} \\ c_{12} e^{m_{12} z} \\ c_{13} e^{m_{13} z} \\ c_{14} e^{m_{14} z} \end{bmatrix} \tag{23}$$

where, m_i is the fourteen eigen values of the problem that is obtained from the characteristic equation as follows

$$[G_1 m^2 + G_2 m + G_3]\{v\} = 0 \tag{24}$$

Due to nonzero vector *v,* the characteristic equation of this problem is obtained by using determinant of the matrix of $[G_1 m^2 + G_2 m + G_3]$:

$$\det[G_1 m^2 + G_2 m + G_3] = 0 \tag{25}$$

Obtained characteristic equation (Eq. (25)) is a fourteen's order equation. By solving the characteristic equation, fourteen roots can be obtained. By substitution of every root m_i in Eq. (24), corresponding fourteen vector v_i may be obtained. ($v^i{}_k$ $(k = 1, 2, ..., 7)$ constitutes the i'th column of Eq. (23) for root m_i). Particular solution of Eq. (19) is

$$[G_3]\{X\}_p = \{F\} \rightarrow \{X\}_p = [G_3]^{-1}\{F\} \tag{26}$$

Therefore, we have the final solution of the problem as follows

$$\{X\} = \{X\}_h + \{X\}_p \tag{27}$$

Two dimensional solution of two ends short circuited cylinder is completed by imposing the appropriate boundary conditions on Eq. (27). For a short-circuited cylinder with clamped-clamped or two simply supported ends, the boundary conditions can be presented as follows, respectively

Clamped-clamped and short circuited

$$\begin{aligned} &u = w = \psi_z = \psi_r = \phi_0 = \phi_1 = \phi_2 = 0 \quad \text{at z=} \tfrac{L}{2}, \\ &\frac{\partial u}{\partial z} = \frac{\partial w}{\partial z} = \frac{\partial \psi_z}{\partial z} = \frac{\partial \psi_r}{\partial z} = \frac{\partial \phi_0}{\partial z} = \frac{\partial \phi_1}{\partial z} = \frac{\partial \phi_2}{\partial z} = 0 \quad \text{at z=0} \end{aligned} \tag{28a}$$

Simply supported and short circuited

$$\begin{aligned} &u = w = \sigma_z = \sigma_\theta = \phi_0 = \phi_1 = \phi_2 = 0 \quad \text{at z=} \tfrac{L}{2}, \\ &\frac{\partial u}{\partial z} = \frac{\partial w}{\partial z} = \frac{\partial \psi_z}{\partial z} = \frac{\partial \psi_r}{\partial z} = \frac{\partial \phi_0}{\partial z} = \frac{\partial \phi_1}{\partial z} = \frac{\partial \phi_2}{\partial z} = 0 \quad \text{at z=0} \end{aligned} \tag{28b}$$

For other boundary conditions, the presented method has capability to solve the problem, exactly.

If we ignore the effect of two end supports of the cylinder, the solution of the system at regions that are adequate far from two ends of the cylinder can be obtained from Eq. (26). This solution can be compared with general solution of FGP cylinder by using the Eq. (27).

3.1 Imposing the boundary condition, Example: clamped-clamped cylinder with two short-circuited ends

Two ends of the cylinder are assumed to be fixed and clamped. Therefore, displacements and rotations vanish at the two ends of the cylinder. Due to imposing the similar boundary condition on the two ends of the cylinder, the slope of the displacements and rotations vanishes at the middle of the cylinder. Eq. (28(a)) implied the mentioned boundary condition of a clamped-clamped cylinder. The electric potential is assumed short-circuited at two ends of the cylinder (Hashemi *et al*. 2010).

It is supposed that all mechanical and electrical components are graded in the radial direction only. Before numerical evaluation, nonhomogeneous properties such as E must be defined as a power function of the radial coordinate as follows (Khoshgoftar *et al*. 2009, arefi and rahimi 2012)

$$E = E_i(\bar{r})^n = E_i(\frac{r}{r_i})^n \xrightarrow{r=R+\rho}$$
$$E = E_i(\bar{r})^n = E_i(\frac{R+\rho}{r_i})^n = \frac{E_i}{r^n{}_i}(R+\rho)^n \quad (29)$$

The values of inner and outer radius and length of the cylinder are selected consistent with reference (Khoshgoftar *et al*. 2009)

$$r_i = 0.6\ ,\ r_0 = 1\ ,\ \mathrm{L}/2 = 15$$

Other numerical values are (Khoshgoftar *et al*. 2009)

C_{zzzz} = 79.2 *Gpa*, C_{zzrr}= C_{rrzz} =45.2 *Gpa*, C_{rrrr} = 83.6 *Gpa*, $C_{rr\theta\theta} = C_{\theta\theta rr}$ = *39.3 Gpa*, $C_{zz\theta\theta}$ $=C_{\theta\theta zz}$ =*45.2 Gpa* $C_{\theta\theta\theta\theta}$ = 74.1 *Gpa*, C_{zrzr} = 79 *Gpa*, e_{rrr} = *0.347(VmN*$^{-1}$*)*, $e_{zzr} = e_{rzz}$ = *-0.16(VmN*$^{-1}$*)*,$e_{\theta\theta r} = e_{r\theta\theta}$ =*-0.16(VmN*$^{-1}$*)*, $\eta_{rr} = 9\times10^{-11}\,(mN^{-1})$ (30)

Table 1 comparison between the present results with solution of previous theories (radial displacement)

r	Theories	n=0	n=1	n=-1	n=2	n=-2
0.6	Present-FSDT	0.00202	0.00158	0.00254	0.00121	0.00313
	Previous- FSDT*	0.00202	0.00157	0.00256	0.00119	0.00316
	Plane elasticity theory	0.00223	0.00177	0.00275	0.00130	0.00334
0.7	Present-FSDT	0.001899	0.00148	0.00238	0.00113	0.00292
	Previous- FSDT [2]	0.001897	0.00147	0.00239	0.00112	0.00295
	Plane elasticity theory	0.00200	0.00157	0.00250	0.00121	0.00305
0.8	Present-FSDT	0.00177	0.00138	0.00221	0.00106	0.00272
	Previous- FSDT [2]	0.00177	0.00137	0.00222	0.00104	0.00274
	Plane elasticity theory	0.00181	0.00142	0.00229	0.00113	0.00284
0.9	Present-FSDT	0.00164	0.00128	0.00205	0.00098	0.00251
	Previous- FSDT [2]	0.00164	0.00127	0.00206	0.00097	0.00253
	Plane elasticity theory	0.00170	0.00131	0.00220	0.00106	0.00267
1	Present-FSDT	0.00151	0.00118	0.00188	0.00091	0.00230
	Previous- FSDT [2]	0.00151	0.00118	0.00189	0.00090	0.00232
	Plane elasticity theory	0.00164	0.00126	0.00208	0.00100	0.00250

* - These results are evaluated by disregarding the first and second order terms of Eq. (19).

4. Results and discussion

4.1. Validation, comparison of the present results with the results of previous theories

The results of this paper were obtained analytically by consideration of the homogeneous and particular solution of the Eq. (19) and imposing the boundary condition Eq. (28(a)). The obtained results can be compared with the previous results at the regions that are adequate far from the two ends of the cylinder and with results of plane elasticity theory (PET). These results are achieved with ignoring the first and second order derivatives in Eq. (19). For comparison of the present results with previous results, radial distribution of the radial displacement is selected.

Table 1 presents the comparison between radial displacements of the present results with the other previous results (Khoshgoftar *et al*. 2009). The mentioned results and comparisons are plotted in Fig 2.

This table indicates that the differences between three methods are not significant at regions that are adequate far from two ends of the cylinder. Hence, the present results and comparisons indicate that employed method has sufficient capability to simulate two dimensional electro elastic analysis of a FGP cylindrical shell. The comparison between the achieved results for validation of the present results can be completed with presentation of the electric displacement along the thickness direction for three methods.

Table 2 comparison between the present results with solution of previous theories (electric potential)

r	Theories	n=0	n=1	n=-1	n=2	n=-2
0.6	Present-FSDT	0	0	0	0	0
	Previous- FSDT[†]	0	0	0	0	0
	Plane elasticity theory	0	0	0	0	0
0.7	Present-FSDT	-118933	-90694	-152508	-70691	-172152
	Previous- FSDT [3]	-118872	-91611	-150844	-69039	-187306
	Plane elasticity theory	-118114	-91348	-147146	-67863	-177151
0.8	Present-FSDT	-158577	-120926	-203344	-94254	-229536
	Previous- FSDT [3]	-158497	-122148	-201125	-92052	-249741
	Plane elasticity theory	-136370	-101336	-176951	-72483	-221832
0.9	Present-FSDT	-118933	-90694	-152508	-70691	-172152
	Previous- FSDT [3]	-118872	-91611	-150844	-69039	-187306
	Plane elasticity theory	-90045	-64589	-121288	-44723	-158037
1	Present-FSDT	0	0	0	0	0
	Previous- FSDT [3]	0	0	0	0	0
	Plane elasticity theory	0	0	0	0	0

[†] - These results are evaluated by disregarding the first and second order terms of Eq. (19).

Table 2 presents the comparison between electric potential of the present results with the other previous results (Khoshgoftar *et al*. 2009). The mentioned results and comparisons are plotted in Fig. 3.

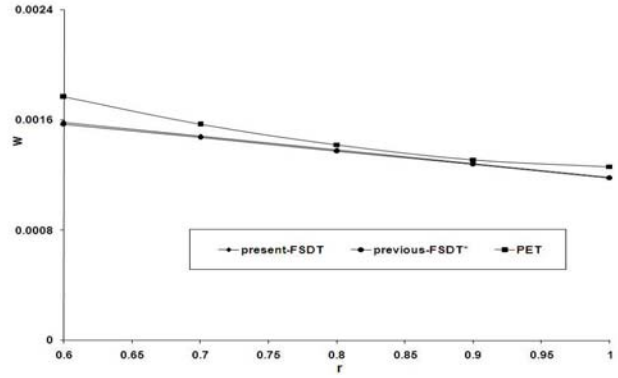

Fig. 2 Comparing the present results (solution of Eq. (19)) with the previous results (solution of Eq. (26)) and plane elasticity solutions for *n=1*

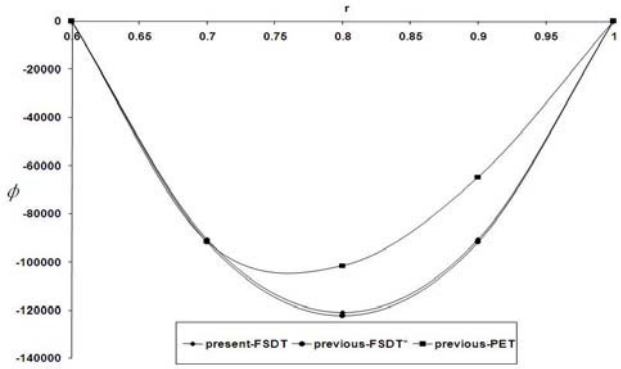

Fig. 3 Comparing present results (solution of Eq. (19)) with the previous results (solution of Eq. (26)) and plane elasticity solutions for *n=1*

4.2. Mechanical and electrical responses

In the present section, the mechanical and electrical responses of a clamped-clamped FGP cylinder can be presented and investigated. These responses can be employed for evaluating the effect of end supports on the longitudinal distribution of mechanical and electrical components. The present results can be compared with those results derived without consideration of the end supports and furthermore with results of plane elasticity theory. Because of symmetric boundary conditions, the achieved results are presented for semi-length of the cylinder. *x=0* is located at the middle of cylinder for whole figures.

Fig. 4 shows the axial distribution of the axial displacement of the mid-surface of the cylinder. The previous researches using the plane elasticity theory has not been had capability to simulate

the end supports effect and then simulates the axial distribution of the axial displacement. This figure indicates that the amplitude of the axial displacement increases with decreasing the nonhomogeneous index '*n*'. The end supports has effect on the distribution of the axial displacement at 15 percent of length of the cylinder. At other regions of the cylinder, the distribution of the mechanical and electrical components is approximately uniform and is independent of the end supports.

Fig. 5 shows the axial distribution of the radial displacement for the mid-surface of the cylinder. This figure indicates that the amplitude of the radial displacement increases with decreasing the nonhomogeneous index 'n'. The end supports has a significant effect on distribution of the axial displacement at 15 percent of length of the cylinder. At other regions of cylinder, the distribution is uniform and is independent of end supports.

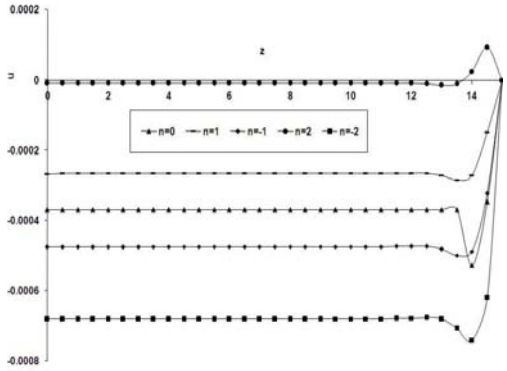

Fig. 4 The axial displacement of mid-plane of the cylinder along the length of the cylinder

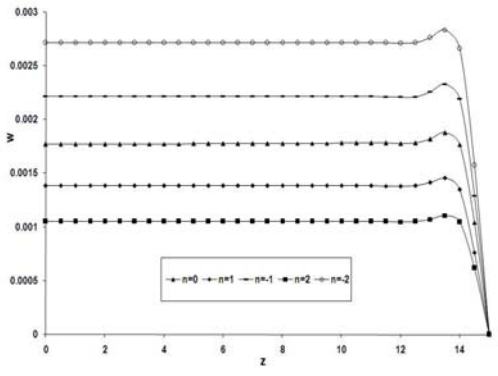

Fig. 5 The radial displacement of mid-plane of the cylinder along the length of the cylinder

The value of rotation about two circumferential and radial axes of the cylinder (ψ_r, ψ_z) can be presented as a main result of the present paper. Fig. 6 shows the axial distribution of the circumferential rotation of the cylinder. This figure indicates that the amplitude of rotation is zero at regions that are adequate far from two ends of the cylinder. At regions near two ends of the

cylinder, the value of rotation is significant. This result is very important in analysis of structures with end supports. The presence of circumferential rotation justifies the presence of shear stress in the structure. A comprehensive review of literature indicates that using the two dimensional plane elasticity theory, calculation of shear stress and radial and axial deformation is not consistent with actual boundary conditions (Jabbari *et al*. 2009). Furthermore the shear stress and strain can not be considered in one dimensional plane elasticity theory. Hence, the present results are very significant in mechanical design especially for evaluation of the shear stress.

Fig. 7 shows the axial distribution of longitudinal rotation. This figure indicates that the value of axial rotation increases with decreasing the value of nonhomogeneous index. The end supports has effect on the uniformly distribution of radial rotation at regions near two end supports.

Fig. 8 shows the axial distribution of maximum electric potential at mid-surface of the cylindrical shell. This figure indicates that the maximum electric potential decreases with increasing the nonhomogeneous index. The electric potential changes abruptly for entire value of nonhomogeneous indexes at near of the end of the cylinder.

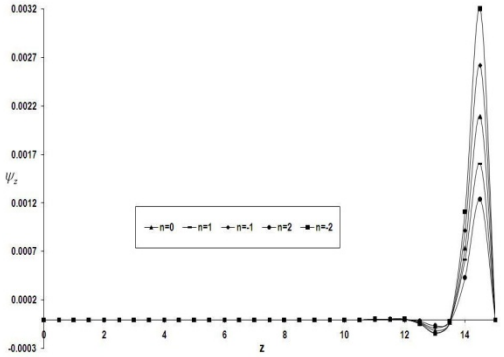

Fig. 6 The circumferential rotation of mid-plane of the cylinder along the length of the cylinder

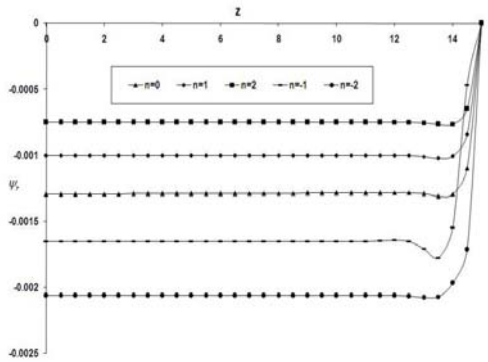

Fig. 7 The radial rotation of mid-plane of the cylinder along the length of the cylinder

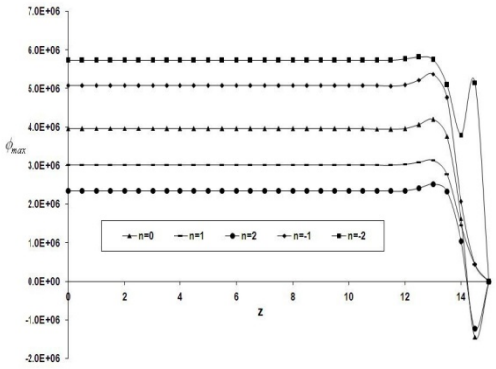

Fig. 8 The axial distribution of maximum electric potential along the length of the cylinder

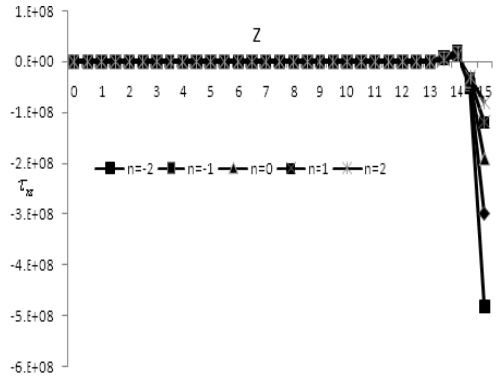

Fig. 9 The axial distribution of shear stress along the length of the cylinder

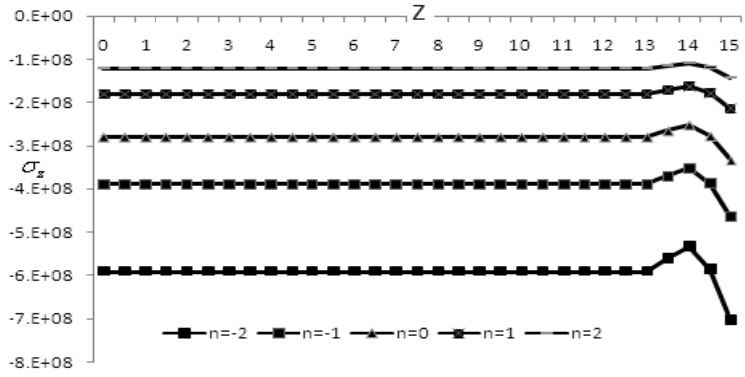

Fig. 10 The axial distribution of axial stress along the length of the cylinder

The axial distributions of shear and axial stress are presented in Figs. 9 and 10 respectively. Fig. 9 indicates that the shear stress is zero at entire length of the cylinder except 15% of both ends of

the cylinder. This result expresses that the magnitude of shear stress is significant at mentioned region. From Fig. 9, same range of effect of end supports can be understood. Abrupt changes of axial stress can be detected at near of two ends of the cylinder.

5. Conclusions

FSDT has been employed for simulation of displacement filed in order to two dimensional analysis of the FGP cylindrical shells. A second order distribution has been employed for electric potential distribution. Final governing differential equation has been solved for clamped-clamped short circuited cylindrical shell. Some important conclusions are expressed as follows:

1. Electro-elastic formulation of a functionally graded piezoelectric cylindrical shell is derived in the present paper. The achieved governing differential equations are second order with seven unknown functions (Four mechanical and three electrical components). The obtained governing equations may be analytically solved for different boundary conditions.
2. Due to imposing the actual mechanical and electrical boundary conditions, it is observed that the responses of the system at near of the two ends of the cylinder change abruptly. These changes tend to significant shear stress at the ends of the cylinder. The previous studies have not had capability to simulate the end effects of the cylinder; exactly and therefore the obtained results have not been had sufficient consistency with actual boundary conditions (Jabbari *et al*. 2009).
3. The obtained differential equation can be solved at regions that are adequate far from two ends of the cylinder. The comprehensive solution of the problem (solution of Eq. (19)) can be compared with solution at those regions (solution of Eq. (26)). This comparison justifies that the present theory (first order shear deformation theory) can be employed as a valid and reasonable theory for analysis of a functionally graded piezoelectric structure.
4. The distribution of different mechanical and electrical components indicates that the absolute value of those components decreases with increasing the value of non-homogenous index.

Acknowledgements

The authors would like to gratefully acknowledge the financial support by University of Kashan. Grant Number:263475/15.

References

Akbarzadeh, A.H., Babaei, M.H. and Chen, Z.T. (2011a), “Thermopiezoelectric analysis of a functionally graded piezoelectric medium”, *Int. J. Appl. Mech.- T ASME*, **3**(1), 47- 68.

Akbarzadeh, A.H., Babaei, M.H. and Chen, Z.T. (2011b), “The thermo-electromagnetoelastic behavior of a rotating functionally graded piezoelectric cylinder”, *Smart. Mater. Struct*., **20**(6), 065008.

Alibeigloo, A. (2010), “Thermoelastic solution for static deformations of functionally graded cylindrical shell bonded to thin piezoelectric layers”, *Compos. Struct*., **93**(2), 961-972.

Arefi, M. and Rahimi, G.H. (2010), “Thermo elastic analysis of a functionally graded cylinder under internal pressure using first order shear deformation theory”, *Sci. Res. Essays*., **5**(12), 1442-1454.

Arefi, M., Rahimi, G.H. and Khoshgoftar, M.J. (2011), "Optimized design of a cylinder under mechanical, magnetic and thermal loads as a sensor or actuator using a functionally graded piezomagnetic material", *Int. J. Phys. Sci*., **6**(27), 6315-6322.

Arefi, M. and Rahimi, G.H. (2011a), "General formulation for the thermoelastic analysis of an arbitrary structure made of functionally graded piezoelectric materials, based on the energy method", *Mech. Eng*., **62**(4), 221-236.

Arefi, M. and Rahimi, G.H. (2011b), "Non linear analysis of a functionally graded square plate with two smart layers as sensor and actuator under normal pressure", *Smart. Struct. Syst*., **8**(5), 433-446.

Arefi, M. and Rahimi, G.H. (2012a), "Studying the nonlinear behavior of the functionally graded annular plates with piezoelectric layers as a sensor and actuator under normal pressure", *Smart. Struct. Syst*., **9**(2), 127-143.

Arefi, M. and Rahimi, G.H. (2012b), "Three-dimensional multi-field equations of a functionally graded piezoelectric thick shell with variable thickness, curvature and arbitrary nonhomogeneity", *Acta. Mech*., **223**(3), 63-79.

Arefi, M. and Rahimi, G.H. (2012c), "The effect of nonhomogeneity and end supports on the thermo elastic behavior of a clamped-clamped FG cylinder under mechanical and thermal loads", *Int. J. Pres. Ves. Pip*., **96**-**97**, 30-37.

Arefi, M. and Rahimi, G.H. (2012d), "Comprehensive thermoelastic analysis of a functionally graded cylinder with different boundary conditions under internal pressure using first order shear deformation theory", *Mechanika*., **18**(1), 5-13.

Arefi, M., Rahimi, G.H. and Khoshgoftar, M.J. (2012e), "Electro elastic analysis of a pressurized thick-walled functionally graded piezoelectric cylinder using the first order shear deformation theory and energy method" , *Mechanika*., **18**(3), 292-300.

Arefi, M., Rahimi, G.H. and Khoshgoftar, M.J. (2012f), "Exact solution of a thick walled functionally graded piezoelectric cylinder under mechanical, thermal and electrical loads in the magnetic field", *Smart. Struct. Syst*., **9**(5), 427-439.

Babaei, M.H. and Chen, Z.T.(2010a),"Transient thermopiezoelectric response of a one-dimensional functionally graded piezoelectric medium to a moving heat source", *Arch. Appl. Mech*., **80 (7)**, 803 - 813.

Babaei, M.H. and Chen, Z.T. (2010b), "Transient hyperbolic heat conduction in a functionally graded hollow cylinder", *J. Thermophys. Heat. Tr*., **24**(2), 325-330.

Babaei, M.H. and Chen, Z.T. (2010c), "The transient coupled thermopiezoelectric response of a functionally graded piezoelectric hollow cylinder to dynamic loadings", *P. Roy. Soc. A - Math. Phy*., **466**, 1077-1091.

Babaei, M.H. and Chen, Z.T. (2008a), "Analytical solution for the electromechanical behavior of a rotating functionally graded piezoelectric hollow shaft", *Arch. Appl. Mech.*, **78**, 489-500.

Babaei, M.H. and Chen, Z.T. (2008b), "Exact solutions for radially polarized and magnetized magnetoelectroelastic rotating cylinders", *Smart. Mater. Struct*., **17**, 025035 (11pp).

Chen, W.Q., Lu, Y., Ye, J.R. and Cai, J.B. (2002), "3D electroelastic fields in a functionally graded piezoceramic hollow sphere under mechanical and electric loading", *Arch. Appl. Mech*., **72**, 39-51.

Dai, H.L., Fu, Y.M. and Yang, J.H. (2007), "Electromagnetoelastic behaviors of functionally graded piezoelectric solid cylinder and sphere", *Acta. Mech. Solida. Sin*., **23**, 55-63.

H-Hashemi, Sh., Es'haghi, M. and Taher, H.R.D. (2010), "An exact nalytical solution for freely vibrating piezoelectric coupled circular/annular thick plates using Reddy plate theory", *Compos. Struct*., **92**(6), 1333-1351.

Jabbari, M., Sohrabpour, S. and Eslami, M.R. (2002), "Mechanical and thermal stresses in a functionally graded hollow cylinder due to radially symmetric loads", *Int. J. Pres. Ves. Pip*., **79**, 493-497.

Jabbari, M., Bahtui, A. and Eslami, M.R. (2009), "Axisymmetric mechanical and thermal stresses in thick short length FGM cylinders", *Int. J. Pres. Ves. Pip*., **86**, 296-306.

Khoshgoftar, M.J., Arani, A.G. and Arefi, M. (2009) "Thermoelastic analysis of a thick walled cylinder made of functionally graded piezoelectric material", *Smart. Mater. Struct*., **18**, 115007 (8 pp).

Liu, X., Wang, Q. and Quek, S.T. (2002), "Analytical solution for free vibration of piezoelectric coupled moderately thick circular plates", *Int. J. Solids. Strutct*., **39**(8), 2129-2151.

Lu, P., Lee, H.P. and Lu, C. (2005), "An exact solution for functionally graded piezoelectric laminated in cylindrical bending", *Int. J. Mech. Sci*., **47**(3), 437-458.
Mirsky, I. and Hermann, G. (1958), "Axially motions of thick cylindrical shells", *J. Appl. Mech. - T ASME*, **25**, 97-102.
Naghdi, P.M. and Cooper, R.M. (1956), "Propagation of elastic waves in cylindrical shells including the effects of transverse shear and rotary inertia", *J. Acoust Soc. Am*., **28**, 56-63.
Peng-Fei, H. and Andrew, Y.T. (2004) "The transient responses of magneto-electro-elastic hollow cylinders", *Smart. Mater. Struct*., **13**(4), 762-776.
Qian, Z.H., Jin, F., Lu, T. and Kishimoto, K, (2008), "Transverse surface waves in functionally graded piezoelectric materials with exponential variation", *Smart, Mater, Struct*., **17**, 065005 (7pp).
Qian, Z.H., Jin, F., Kishimoto, K. and Lu, T.J. (2009), "Propagation behavior of Love waves in a functionally graded half-space with initial stress", *Int. J. Solids. Struct.*, **46**,1354-1361.
Qian, Z.H., Jin, F. and Hirose S. (2011a), "Effects of covering layer thickness on Love waves in functionally graded piezoelectric substrates", *Arch. Appl. Mech*., **81**(11), 1743-1755.
Qian, Z.H., Jin, F. and Hirose, S. (2011b), "Piezoelectric Love waves in an FGPM layered structure", *Mech. Adv. Mater. Struct*., **18**(1), 77-84.
Qian, Z.H., Jin, F., Lu, T.J. and Kishimoto, K. (2009), "Transverse surface waves in a functionally graded piezoelectric substrate coated with a finite-thickness metal waveguide layer", *Appl. Phy. Lett*., **94**(2), 023501.
Qian, Z.H., Jin, F., Hirose, S. and Lu, T.J. (2009), "Effects of material gradient on transverse surface waves in piezoelectric coupled solid media", *Appl. Phy. Lett*., **95**(7), 073501.
Qian, Z.H., Jin, F., Lu, T.J. and Kishimoto, K. (2009), "Transverse surface waves in a layered structure with a functionally graded piezoelectric substrate and a hard dielectric layer", *Ultrasonics*, **49**(3), 293-297.
Rahimi, G.H., Arefi, M. and Khoshgoftar, M.J. (2011), "Application and analysis of functionally graded piezoelectrical rotating cylinder as mechanical sensor subjected to pressure and thermal loads", *Appl. Math. Mech. - Eng*., **32**(8), 997-1008.
Shi, Z.F. and Chen, Y. (2004), "Functionally graded piezoelectric cantilever beam under load", *Arch. Appl. Mech*., **74**(3-4), 237-247.
Shao, Z.S. (2005), "Mechanical and thermal stresses of a functionally graded circular hollow cylinder with finite length", *Int. J. Pres. Ves. Pip*., **82**(3), 155-163.
Sheng, G.G. and Wang, X. (2010), "Thermoelastic vibration and buckling analysis of functionally graded piezoelectric cylindrical shells", *Appl. Math. Model*., **34**(9), 2630-2643.
Timoshenko, S.P. (1976), *Strength of Materials*, Part II (Advanced Theory and Problems), 3rd Ed., Van Nostrand Reinhold Co, New York.
Tutuncu, N. and Ozturk, M. (2001), "Exact solution for stresses in functionally graded pressure vessels", *Compos. Part B - Eng*., **32**(8), 683-686.
Wu, L., Zhiqing, J. and Jun, L. (2005), "Thermoelastic stability of functionally graded cylindrical shells". *Compos. Struct*., **70**(1), 60-68.
Wang, H.M. and Xu, Z.X. (2010), "Effect of material inhomogeneity on electromechanical behaviors of functionally graded piezoelectric spherical structures", *Comput. Mater. Sci*., **48**(2), 440-445.
Yamanouchi, M, Koizumi, M. and Shiota, I. (1990), *Proceedings of the 1st International Symposium on Functionally Gradient Materials*, Sendai, Japan.

CC

Appendix A

$$U_S = \sum_{i=1}^{9} A_i(z) f_i(z)$$

$$A_1(z) = \int_{-\frac{h}{2}}^{\frac{h}{2}} (R+\rho) C_{zzzz} d\rho, A_2(z) = \int_{-\frac{h}{2}}^{\frac{h}{2}} \rho(R+\rho) C_{zzzz} d\rho, A_3(z) = \int_{-\frac{h}{2}}^{\frac{h}{2}} \rho^2 (R+\rho) C_{zzzz} d\rho, A_4(z) = \int_{-\frac{h}{2}}^{\frac{h}{2}} C_{zz\theta\theta} d\rho$$

$$A_5(z) = \int_{-\frac{h}{2}}^{\frac{h}{2}} \rho C_{zz\theta\theta} d\rho, A_6(z) = \int_{-\frac{h}{2}}^{\frac{h}{2}} \rho^2 C_{zz\theta\theta} d\rho, A_7(z) = \int_{-\frac{h}{2}}^{\frac{h}{2}} (R+\rho) C_{zzrr} d\rho, A_8(z) = \int_{-\frac{h}{2}}^{\frac{h}{2}} \rho(R+\rho) C_{zzrr} d\rho$$

$$A_9(z) = \int_{-\frac{h}{2}}^{\frac{h}{2}} C_{zz\theta\theta} d\rho,\ A_{10}(z) = \int_{-\frac{h}{2}}^{\frac{h}{2}} \rho C_{rr\theta\theta} d\rho, A_{11}(z) = \int_{-\frac{h}{2}}^{\frac{h}{2}} \frac{C_{\theta\theta\theta\theta}}{R+\rho} d\rho, A_{12}(z) = \int_{-\frac{h}{2}}^{\frac{h}{2}} \frac{\rho C_{\theta\theta\theta\theta}}{R+\rho} d\rho, A_{13}(z) = \int_{-\frac{h}{2}}^{\frac{h}{2}} \frac{\rho^2 C_{\theta\theta\theta\theta}}{R+\rho} d\rho$$

$$A_{14}(z) = \int_{-\frac{h}{2}}^{\frac{h}{2}} (R+\rho) C_{rrrr} d\rho, A_{15}(z) = \int_{-\frac{h}{2}}^{\frac{h}{2}} C_{rzrz} (R+\rho) d\rho, A_{16}(z) = \int_{-\frac{h}{2}}^{\frac{h}{2}} \rho C_{rzrz} (R+\rho) d\rho, A_{17}(z) = \int_{-\frac{h}{2}}^{\frac{h}{2}} \rho^2 C_{rzrz} (R+\rho) d\rho$$

Appendix B

$$U(z)_{Piezo} = \sum_{i=1}^{32} C_i(z) I_i(u, w, \psi_z, \psi_r, \phi_0, \phi_1, \phi_2, z) =$$

$$C_1 = \int_{-\frac{h}{2}}^{\frac{h}{2}} e_{zzz}(R+\rho) d\rho], C_2 = \int_{-\frac{h}{2}}^{\frac{h}{2}} \rho e_{zzz}(R+\rho) d\rho, C_3 = \int_{-\frac{h}{2}}^{\frac{h}{2}} \rho^2 e_{zzz}(R+\rho) d\rho, C_4 = \int_{-\frac{h}{2}}^{\frac{h}{2}} \rho^3 e_{zzz}(R+\rho) d\rho, C_5 = \int_{-\frac{h}{2}}^{\frac{h}{2}} e_{rrr}(R+\rho) d\rho$$

$$C_6 = \int_{-\frac{h}{2}}^{\frac{h}{2}} e_{rrr} \rho(R+\rho) d\rho, C_7 = \int_{-\frac{h}{2}}^{\frac{h}{2}} e_{zzr}(R+\rho) d\rho, C_8 = \int_{-\frac{h}{2}}^{\frac{h}{2}} e_{zzr} \rho(R+\rho) d\rho, C_9 = \int_{-\frac{h}{2}}^{\frac{h}{2}} e_{zzr} \rho^2 (R+\rho) d\rho, C_{10} = \int_{-\frac{h}{2}}^{\frac{h}{2}} e_{rzz}(R+\rho) d\rho,$$

$$C_{11} = \int_{-\frac{h}{2}}^{\frac{h}{2}} e_{rzz} \rho(R+\rho) d\rho, C_{12} = \int_{-\frac{h}{2}}^{\frac{h}{2}} e_{rzz}(R+\rho) \rho^2 d\rho, C_{13} = \int_{-\frac{h}{2}}^{\frac{h}{2}} e_{rrz}(R+\rho) d\rho, C_{14} = \int_{-\frac{h}{2}}^{\frac{h}{2}} e_{rrz} \rho(R+\rho) d\rho, C_{15} = \int_{-\frac{h}{2}}^{\frac{h}{2}} e_{rrz}(R+\rho) \rho^2 d\rho$$

$$C_{16} = \int_{-\frac{h}{2}}^{\frac{h}{2}} e_{zrr}(R+\rho) d\rho, C_{17} = \int_{-\frac{h}{2}}^{\frac{h}{2}} e_{zrr} \rho(R+\rho) d\rho, C_{18} = \int_{-\frac{h}{2}}^{\frac{h}{2}} e_{zrr}(R+\rho) \rho^2 d\rho, C_{19} = \int_{-\frac{h}{2}}^{\frac{h}{2}} e_{\theta\theta z} d\rho, C_{20} = \int_{-\frac{h}{2}}^{\frac{h}{2}} e_{\theta\theta z} \rho d\rho, C_{21} = \int_{-\frac{h}{2}}^{\frac{h}{2}} e_{\theta\theta z} \rho^2 d\rho$$

$$C_{22} = \int_{-\frac{h}{2}}^{\frac{h}{2}} e_{\theta\theta z} \rho^3 d\rho, C_{23} = \int_{-\frac{h}{2}}^{\frac{h}{2}} e_{z\theta\theta} d\rho, C_{24} = \int_{-\frac{h}{2}}^{\frac{h}{2}} e_{z\theta\theta} \rho d\rho, C_{25} = \int_{-\frac{h}{2}}^{\frac{h}{2}} e_{z\theta\theta} \rho^2 d\rho, C_{26} = \int_{-\frac{h}{2}}^{\frac{h}{2}} e_{z\theta\theta} \rho^3 d\rho, C_{27} = \int_{-\frac{h}{2}}^{\frac{h}{2}} e_{\theta\theta r} d\rho, C_{28} = \int_{-\frac{h}{2}}^{\frac{h}{2}} e_{\theta\theta r} \rho d\rho$$

$$C_{29} = \int_{-\frac{h}{2}}^{\frac{h}{2}} e_{\theta\theta r} \rho^2 d\rho, C_{30} = \int_{-\frac{h}{2}}^{\frac{h}{2}} e_{r\theta\theta} d\rho, C_{31} = \int_{-\frac{h}{2}}^{\frac{h}{2}} e_{r\theta\theta} \rho d\rho, C_{32} = \int_{-\frac{h}{2}}^{\frac{h}{2}} e_{r\theta\theta} \rho^2 d\rho$$

Appendix C

$$U_{Die}(z)=\sum_{i=1}^{16} D_i(z)J_i(\phi_0,\phi_1,\phi_2,z)=$$

$$D_1=\int_{-\frac{h}{2}}^{\frac{h}{2}}\eta_{zz}(R+\rho)d\rho, D_2=\int_{-\frac{h}{2}}^{\frac{h}{2}}\eta_{zz}\rho(R+\rho)d\rho, D_3=\int_{-\frac{h}{2}}^{\frac{h}{2}}\eta_{zz}\rho^2(R+\rho)d\rho, D_4=\int_{-\frac{h}{2}}^{\frac{h}{2}}\eta_{zz}\rho^3(R+\rho)d\rho$$

$$D_5=\int_{-\frac{h}{2}}^{\frac{h}{2}}\eta_{zz}\rho^4(R+\rho)d\rho, D_6=\int_{-\frac{h}{2}}^{\frac{h}{2}}\eta_{zr}(R+\rho)d\rho, D_7=\int_{-\frac{h}{2}}^{\frac{h}{2}}\eta_{zr}\rho(R+\rho)d\rho, D_8=\int_{-\frac{h}{2}}^{\frac{h}{2}}\eta_{zr}\rho^2(R+\rho)d\rho$$

$$D_9=\int_{-\frac{h}{2}}^{\frac{h}{2}}\eta_{zr}\rho^3(R+\rho)d\rho, D_{10}=\int_{-\frac{h}{2}}^{\frac{h}{2}}\eta_{rz}(R+\rho)d\rho, D_{11}=\int_{-\frac{h}{2}}^{\frac{h}{2}}\eta_{rz}\rho(R+\rho)d\rho, D_{12}=\int_{-\frac{h}{2}}^{\frac{h}{2}}\eta_{rz}\rho^2(R+\rho)d\rho$$

$$D_{13}=\int_{-\frac{h}{2}}^{\frac{h}{2}}\eta_{rz}\rho^3(R+\rho)d\rho, D_{14}=\int_{-\frac{h}{2}}^{\frac{h}{2}}\eta_{rr}(R+\rho)d\rho, D_{15}=\int_{-\frac{h}{2}}^{\frac{h}{2}}\eta_{rr}\rho(R+\rho)d\rho, D_{16}=\int_{-\frac{h}{2}}^{\frac{h}{2}}\eta_{rr}\rho^2(R+\rho)d\rho$$

Appendix D

$$F=\begin{Bmatrix}0\\0\\2(P_i(R-\frac{h}{2})-P_0(R+\frac{h}{2}))\\2\frac{h}{2}(-P_i(R-\frac{h}{2})-P_0(R+\frac{h}{2}))\\0\\0\\0\end{Bmatrix}$$

Appendix E

$$G_1=\begin{Bmatrix}2(1-\nu)A_1 & 2(1-\nu)A_2 & 0 & 0 & 2C_1 & 2C_2 & 2C_3\\ -2(1-\nu)A_2 & -2(1-\nu)A_3 & 0 & 0 & 2C_2 & -2C_3 & -2C_4\\ 0 & 0 & -(1-2\nu)A_1 & -(1-2\nu)A_2 & 0 & 0 & 0\\ 0 & 0 & -(1-2\nu)A_2 & -(1-2\nu)A_3 & 0 & 0 & 0\\ 2C_1 & 2C_2 & 0 & 0 & -2D_1 & -2D_2 & -2D_3\\ -2C_2 & -2C_3 & 0 & 0 & 2D_2 & 2D_3 & 2D_4\\ -2C_3 & -2C_4 & 0 & 0 & 2D_3 & 2D_4 & 2D_5\end{Bmatrix}_{7\times 7}$$

Appendix F

$$G_2 = \begin{Bmatrix} 0 & 0 & 2vA_4 & 2v(A_1+A_6) & 0 & C_7+C_{10} & 2(C_8+C_{11}) \\ 0 & 0 & A_1\times(1-2v)-2vA_6 & (1-4v)A_2-2vA_9 & 0 & -(C_8+C_{11}) & -2(C_9+C_{12}) \\ 2vA_4 & 2vA_6-A_1\times(1-2v) & 0 & 0 & (C_{19}+C_{23}) & (C_{20}+C_{24}) & (C_{21}+C_{25}) \\ 2v(A_1+A_6) & 2vA_9-A_2(1-4v) & 0 & 0 & (C_{13}+C_{16}+C_{20}+C_{24}) & (C_{14}+C_{17}+C_{21}+C_{25}) & (C_{15}+C_{18}+C_{22}+C_{26}) \\ 0 & 0 & (C_{19}+C_{23}) & (C_{13}+C_{16}+C_{20}+C_{24}) & 0 & -(D_6+D_{10}) & -2(D_7+D_{11}) \\ (C_7+C_{10}) & (C_8+C_{11}) & -(C_{20}+C_{24}) & -(C_{14}+C_{17}+C_{21}+C_{25}) & -(D_6+D_{10}) & 0 & (D_8+D_{12}) \\ 2(C_8+C_{11}) & 2(C_9+C_{12}) & -(C_{21}+C_{25}) & -(C_{15}+C_{18}+C_{22}+C_{26}) & -2(D_7+D_{11}) & -(D_8+D_{12}) & -(D_9+D_{13}) \end{Bmatrix}_{7\times7}$$

Appendix G

$$G_3 = \begin{Bmatrix} 0 & 0 & 0 & 0 & 0 & 0 & 0 \\ 0 & (1-2v)A_1 & 0 & 0 & 0 & 0 & 0 \\ 0 & 0 & 2(1-v)A_5 & 2vA_4+2(1-v)A_7 & 0 & (C_{27}+C_{30}) & 2(C_{28}+C_{31}) \\ 0 & 0 & 2(vA_4+(1-v)A_7) & 2\{(1-v)A_1+2vA_6+(1-v)A_8\} & 0 & (2C_5+C_{28}+C_{31}) & (4C_6+2C_{29}+2C_{32}) \\ 0 & 0 & 0 & 0 & 0 & 0 & 0 \\ 0 & 0 & (C_{27}+C_{31}) & (2C_5+C_{28}+C_{31}) & 0 & -2D_{14} & -4D_{15} \\ 0 & 0 & 2(C_{28}+C_{31}) & (4C_6+2C_{29}+2C_{32}) & 0 & -4D_{15} & -8D_{16} \end{Bmatrix}_{7\times7}$$

Nomenclature

b	Radius of an arbitrary layer of cylinder	f_i, I_i, J_i	A function of component of displacements and electric potential
ρ	Coordinate of arbitrary layer of cylinder respect to middle surface	A_i, C_i, D_i	General property of material
R	Radius of mid-surface of cylinder	G	Shear modulus of elasticity
u_z	Axial component of deformation	P_i	Internal pressure
w_r	Radial component of deformation	P_0	External pressure
u	Displacement component of axial deformation	W	External work(due to pressure)
w	Displacement component of radial deformation	C_1	General force
ψ_z	Rotational component of axial deformation	C_2	General moment
ψ_r	Rotational component of radial deformation	F	Functional
ε_z	Axial strain	N_z	Resultant of axial force
ε_r	Radial strain	N_e	Resultant of tangential force
ε_θ	Circumferential strain	N_r	Resultant of radial force
ε_{rz}	Shear strain in xz plane	M_z	Resultant of axial moment
σ_z	Axial stress	M_e	Resultant of tangential moment
σ_r	Radial stress	M_{rz}	Resultant of shear force
σ_θ	Circumferential stress	Q_z	Resultant of axial force
τ_{xz}	Shear stress	$\{Z\}$	Unknown functions
C_{ijkl}	Elastic stiffness coefficient	$[G_1]$	7×7 matrices of material property
e_{ijk}	Piezoelectric coefficient	$[G_2]$	7×7 matrices of material property
ϕ	Electric potential	$[G_3]$	7×7 matrices of material property
U	Total energy	$\{F\}$	Vector of general force
$\bar{u}$	Energy per unit volume	E_i	Modulus of elasticity in the inner radius
dV	Element of volume	r_i	Inner radius
h	Local thickness of cylinder	r_o	Outer radius
U_s	Mechanical strain energy	n	Non homogenous index
U_{piezo}	Piezoelectric energy	L	Length of cylinder
U_{die}	Dielectric energy	d_x, d_z	Resultant of electric displacement